

## RESEARCH ARTICLE

DRUG DEVELOPMENT RESEARCH

WILEY

# Design, synthesis, and biological evaluation of 3',4',5'-trimethoxy evodiamine derivatives as potential antitumor agents

Yijiao Peng<sup>1,2</sup> | Runde Xiong<sup>1,2</sup> | Zhen Li<sup>2</sup> | Junmei Peng<sup>2</sup> | Zhi-Zhong Xie<sup>2</sup>  |  
Xiao-Yong Lei<sup>2</sup> | Dongxiu He<sup>1,2</sup> | Guotao Tang<sup>1,2</sup> 

<sup>1</sup>Institute of Pharmacy and Pharmacology, Hunan Province Cooperative Innovation Center for Molecular Target New Drug Study, University of South China, Hengyang City, China

<sup>2</sup>Hunan Provincial Key Laboratory of Tumor Microenvironment Responsive Drug Research, Hengyang City, Hunan Province, China

## Correspondence

Guotao Tang and Dongxiu He, Hunan Provincial Key Laboratory of Tumour Microenvironment Responsive Drug Research University of South China 28# Chang-Sheng Road, Hengyang City, Hunan Province, 421001, People's Republic of China. Email: tgzq@163.com (G.-T.T.) and hdx711106@126.com (D.-X.H.)

## Funding information

Hunan Postgraduate Research and Innovation Project, Grant/Award Number: CX20190751; Hunan Province Cooperative Innovation Center for Molecular Target New Drug Study, The natural science foundation of hunan province, Grant/Award Number: 2020JJ4534; Hunan Provincial Key Laboratory of Tumor Microenvironment Responsive Drug Research, Grant/Award Number: 2019-56

## Abstract

A series of compounds bearing 3',4',5'-trimethoxy module into the core structure of evodiamine were designed and synthesized. The synthesized compounds were screened *in vitro* for their antitumor potential. MTT results showed that compounds **14a–14c** and **14i–14j** had significant effects, with compound **14h** being the most prominent, with an  $IC_{50}$  value of  $3.3 \pm 1.5 \mu\text{M}$ , which was lower than evodiamine and 5-Fu. Subsequent experiments further confirmed that compound **14h** could inhibit cell proliferation and migration, and induce G2/M phase arrest to inhibit the proliferation of HGC-27 cells, which is consistent with the results of the cytotoxicity experiment. Besides, **14h** could inhibit microtubule assembly and might kill tumor cells by inhibiting VEGF and glycolysis. All experimental results indicate that compound **14h** might be a potential drug candidate for the treatment of gastric cancer and was worthy of further study.

## KEYWORDS

evodiamine, microtubule assembly, trimethoxy benzene

## 1 | INTRODUCTION

The tumor microenvironment plays an important role in the development and progression of tumors, and its main features include low pH, hypoxia, angiogenesis, and abnormal glucose metabolism (Chen et al., 2018; Yang, 2017). When tumors grow beyond a certain size, overexuberant growth requires tumor blood vessels to provide sufficient oxygen and nutrients. The important role of tumor blood vessels in tumor development makes it one of the antitumor targets (Gaya & Rustin, 2005; McKeage & Baguley, 2010; Porcu et al., 2014). Tumor vascular targeted drugs can be divided into two types: angiogenesis

inhibitor (AI) and vascular disrupting agent (VDA). Both preclinical and clinical studies have shown that the combination of AI and VDA can increase antitumor effectiveness (Siemann et al., 2017; Siemann & Shi, 2004).

The synthesis of novel colchicine site tubulin inhibitors based on trimethoxyphenyl has become a research hotspot (Belleri et al., 2005; Li et al., 2018). Some microtubule targeting agents containing TMP structures have been found to inhibit microtubule polymerization and act as effective tumor-VDA against cancer. CA4P (Figure 1) (Liang et al., 2016; Quan et al., 2008; Zhang et al., 2013) and its similar OXi4503 (Bothwell et al., 2016), AVE8062 (Sessa et al., 2013), colchicine analog ZD6126 (LoRusso et al., 2008), BNC-105 (Nowak et al., 2013), CKD-516 (Lee et al., 2010) all have 3,4,5-trimethoxyphenyl

Yijiao Peng and Runde Xiong contributed equally to this study.

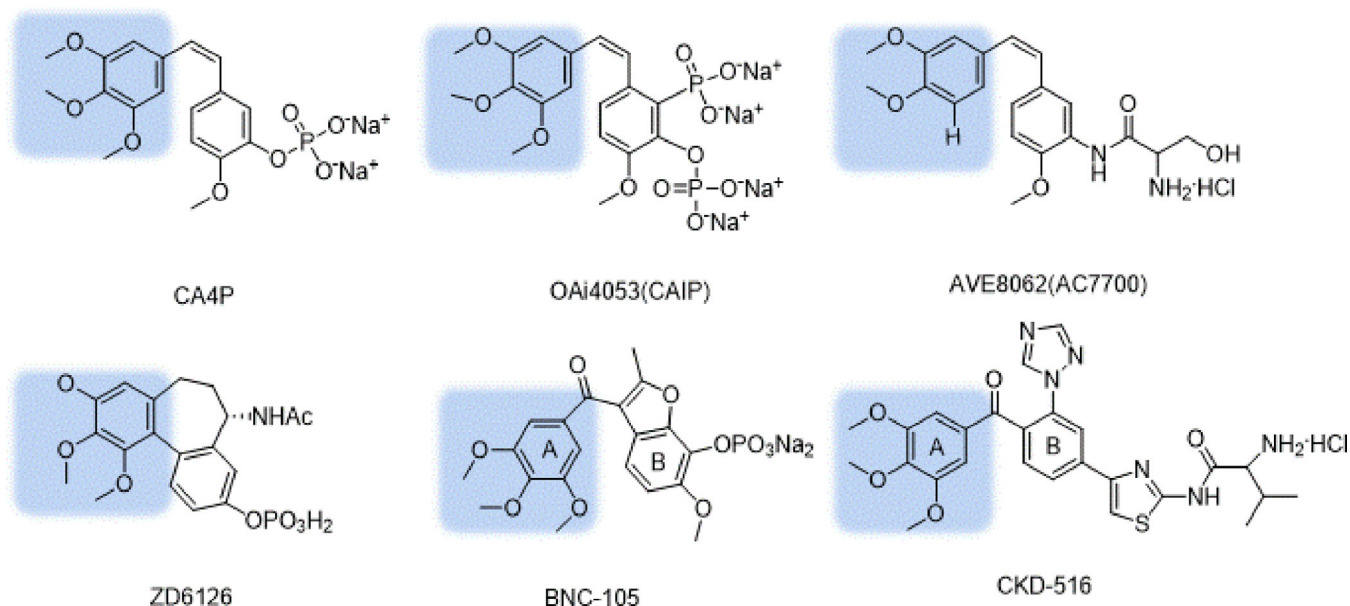


**FIGURE 1** Schematic diagram of the structure of some compounds containing trimethoxyphenyl

scaffold. As a pharmacophore of Tumor-VDA, Trimethoxyphenyl is retained as the necessary active part, and the bridge chain in the middle can be modified with amide bond, sulfonamide bond, and so on (Herdman et al., 2016; Nguyen et al., 2012; Yan et al., 2015).

Evodiamine is an alkaloid extracted from *Evodia* (Tan & Zhang, 2016), which has a wide range of biological activities such as antiinflammatory (Liao et al., 2011), antiobesity (Bak et al., 2010), thermoregulation, and vasodilation (Gavaraskar et al., 2015). In recent years, studies on evodiamine have found that its antitumor function was realized by inhibiting proliferation, blocking the cell cycle, and inducing apoptosis. Evodiamine can inhibit the proliferation of a variety of tumor cells, such as colon cancer cells (Huang et al., 2015; Zhao et al., 2015), human gastric cancer cells (Rasul et al., 2012; Yang et al., 2014), human lung cancer cells (Hong et al., 2014), human hepatic cells (Hu et al., 2017), etc. Evodiamine can significantly block the percentage of tumor cells in the G2/M of the cell cycle. Its mechanism is related to the regulation of the expression of cyclin, CDKs, and cell cycle checkpoint kinases (Fang et al., 2014). In addition, it can also block some tumor cells in the G1 phase by affecting the expression of G1 phase-related proteins and activating the p53-p21-Rb pathway (Chien et al., 2014). In terms of inducing apoptosis, evodiamine can increase the expression of death receptors on the surface of tumor cells and promote the binding of death receptors and ligands, thereby promoting the death signal complex formation and inducing tumor cell apoptosis (Khan et al., 2015). Evodiamine can also change the permeability of the mitochondrial membrane to release cytochrome C and apoptosis-inducing factors into the cytoplasm to induce tumor cell apoptosis (Chen et al., 2016; Jaiswal et al., 2015; Shen et al., 2015).

The most interesting thing is that evodiamine can down-regulate the expression of  $\beta$ -catenin, which leads to a decline of vascular endothelial growth factor (VEGF) at the transcriptional level and affects

VEGF-induced angiogenesis (Huang et al., 2015) indicating that evodiamine may be a potent angiogenesis inhibitor. At the same time, evodiamine can downregulate the expression of PhosphoFructoKinase (PFK) protein, the key enzyme of glucose metabolism, and inhibit the transcription of Hypoxia Inducible Factor (HIF) and AKT genes related to the Warburg effect (Jiang, 2015).

To enhance the blocking effect of evodiamine on tumor vasculature, we have proposed combination principles to modify the structure of evodiamine by introducing the trimethoxy benzene group into the E ring or modify it on indole N atom. Herein, we have synthesized a series of new 3',4',5'-trimethoxy evodiamine derivatives and identified compound **14h** as an applicable drug candidate for antitumor chemotherapy of cancer.

## 2 | MATERIALS AND METHODS

### 2.1 | Chemicals

#### 2.1.1 | Materials and reagents

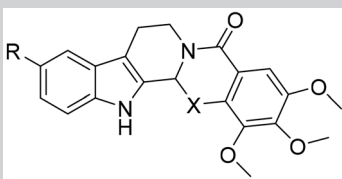
The materials and reagents used in the experiment were purchased through commercial channels and could be used directly without further purification unless otherwise specified. Using thin-layer chromatography (TLC) on a silica gel 60F254 plates, visualizing the results under 254 or 365 nm ultraviolet light as a reference, the compounds were separated using silica gel (200 mesh size) by column chromatography. The melting point of the compound was determined with a Thermo Scientific electrothermal digital melting point instrument (uncorrected). ESI mass spectrometry data was obtained by Waters GCT mass spectrometer. The  $^1\text{H}$  NMR spectrum was measured by Bruker AV-400 spectrometer, and the experiment was carried out in the designated solvent (TMS as internal

standard). The  $\delta$  value (ppm) was used to indicate the chemical shift value, and the Hz was used to indicate the coupling constant ( $J$ ).

## 2.1.2 | Synthesis methods of compound 6a–b and 7a–b

The solution of tryptamine (**1**, 1.60 g, 0.01 mol) in ethyl formate (20 ml) was heated to 60°C, stirred for 6 h, and the compound **2** was obtained after the ethyl formate was removed under reduced pressure. POCl<sub>3</sub> (1 ml) was added to the solution of compound **2** in CH<sub>2</sub>Cl<sub>2</sub> (30 ml) and stirred at 0–5°C for 6 h. The solvent was then removed under reduced pressure. The crude product was purified by the silica gel column (CH<sub>2</sub>Cl<sub>2</sub>:CH<sub>3</sub>OH = 10:1) to obtain **3**. The solution of 2-amino-3,4,5-trimethoxybenzoic acid (**4**, 0.23 g, 1 mmol) and acetyl chloride (0.8 ml) in ethyl chloroformate (15 ml) was heated to 95°C and stirred for 2 h. Cool to room temperature and precipitate compound **5** from the solution.

**TABLE 1** Synthesis of E-ring substituted trimethoxy evodiamine derivatives (**6a**, **6b**, **7a**, and **7b**)



Compound	R	X
<b>6a</b>	–H	NH
<b>6b</b>	–H	=N
<b>7a</b>	–CH <sub>3</sub> O	NH
<b>7b</b>	–CH <sub>3</sub> O	=N

The solution of 3,4-dihydro- $\beta$ -carbene (**3**, 0.17 g, 1 mmol) and **4** (0.25 g, 1 mmol) in CH<sub>2</sub>Cl<sub>2</sub> (20 ml) was stirred at room temperature for 24 h. The crude product was purified by a silica gel column (CH<sub>2</sub>Cl<sub>2</sub>). Compound **6a** (0.38 g, 1 mmol) was added IBX (0.41 g, 1.5 mmol) in DMSO (20 ml) solution and stirred at room temperature for 2 h. Then added water (40 ml) and extracted with ethyl acetate (3  $\times$  30 ml). The composite organic phase was removed under reduced pressure. The crude product was purified by silica gel column (CH<sub>2</sub>Cl<sub>2</sub>) to get **7a–b**.

The compounds are listed in Table 1.

The <sup>1</sup>H NMR data of compounds **6a–6b**, and **7a–7b** were supplied as experiment data (Scheme 1).

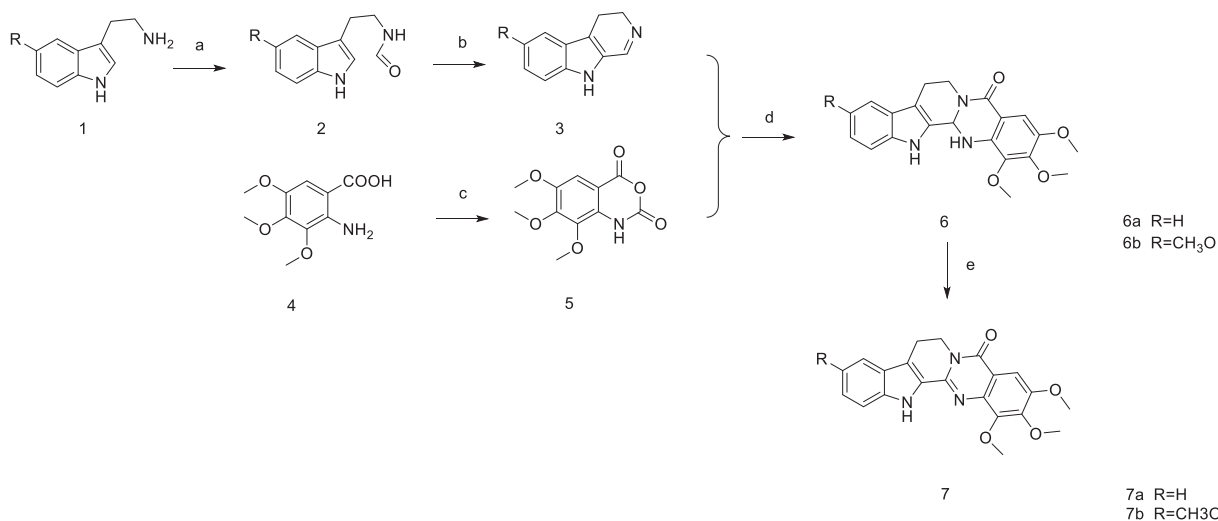
## 2.1.3 | Synthesis methods of compound 14a–n

2-Oxybenzoic acid (**12**, 0.69 g, 5 mmol) was added with thionyl chloride (1.18 g, 10 mmol) in CH<sub>2</sub>Cl<sub>2</sub> (25 ml) solution and stirred at 40°C for 1 h. The solvent was then removed under reduced pressure. The residue was added to the solution of intermediate **3** (0.85 g, 5 mmol) in CH<sub>2</sub>Cl<sub>2</sub> (40 ml) and stirred at room temperature for 24 h. After the reaction, the solvent was removed under reduced pressure, and the crude product was purified by a silica gel column (CH<sub>2</sub>Cl<sub>2</sub>). The intermediate **13** was obtained. NAH (0.05 g, 2 mmol) was added to the solution of compound **13** (0.29 g, 1 mmol) in DMF (20 ml) and stirred at 0°C for 20 min. Then 3,4,5-trimethoxybenzoyl chloride (0.23 g, 1 mmol) was added and stirred at 0–5°C for 24 h. Then add water (40 ml) and precipitate the crude from the solution. The crude product was purified by silica gel column (CH<sub>2</sub>Cl<sub>2</sub>) for **14a**.

The preparation method of compound **14b–n** was similar to the above method.

The compounds are listed in Table 2.

The <sup>1</sup>H NMR and ESI-MS spectra data of compounds **14a–14n** were supplied as experiment data (Scheme 2).



**SCHEME 1** Synthetic route of **6a–b**, **7a–b**

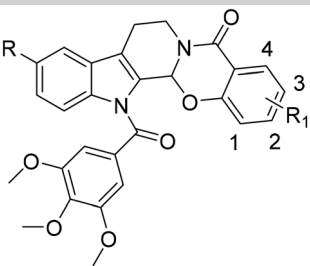
## 2.2 | Cell culture

The Bel-7402, A549, HCT-116, MCF-7, HGC-27, and GES-1 cells used in the experiment were purchased from the Typical Culture Collection Center of the Chinese Academy of Sciences in Shanghai, China. The culture medium used for culturing these cells is configured according to the relevant culture instructions. All cells were cultured in a humidified incubator at 37°C and 5% CO<sub>2</sub>.

## 2.3 | Cytotoxicity test

Detected 18 kinds of trimethoxyphenyl evodiamine derivatives on five tumor cells (Bel-7402, A549, HCT-116, MCF-7, and HGC-27) and a

**TABLE 2** Synthesis of B-ring substituted trimethoxy evodiamine derivatives (14a–14n)



Compound	R	R1
14a	-H	-H
14b	-H	1-CH <sub>3</sub>
14c	-H	2-CH <sub>3</sub>
14d	-H	2-Cl
14e	-H	3-Cl
14f	-H	3-Br
14g	-H	2-NO <sub>2</sub>
14h	-CH <sub>3</sub> O	-H
14i	-CH <sub>3</sub> O	1-CH <sub>3</sub>
14j	-CH <sub>3</sub> O	2-CH <sub>3</sub>
14k	-CH <sub>3</sub> O	2-Cl
14l	-CH <sub>3</sub> O	3-Cl
14m	-CH <sub>3</sub> O	3-Br
14n	-CH <sub>3</sub> O	2-NO <sub>2</sub>

normal cell (GES-1) cytotoxicity. Added the cell suspension to a 96-well plate and waited for the cells to adhere to the wall. After 48 h of incubation with different concentrations of drugs as required, 20 μl MTT was added to each well. After the culture continued for 4 h, the liquid was aspirated and 150 μl DMSO was added. Shaked in the dark for 10 min, and used a Wellsan MK-2 microplate reader to measure the OD value at a wavelength of 490 nm. GraphPad Prism 8.0 software was used to process and analyze the experimental data. All experiments were performed three times independently (Supporting Information).

## 2.4 | Cell migration experiment

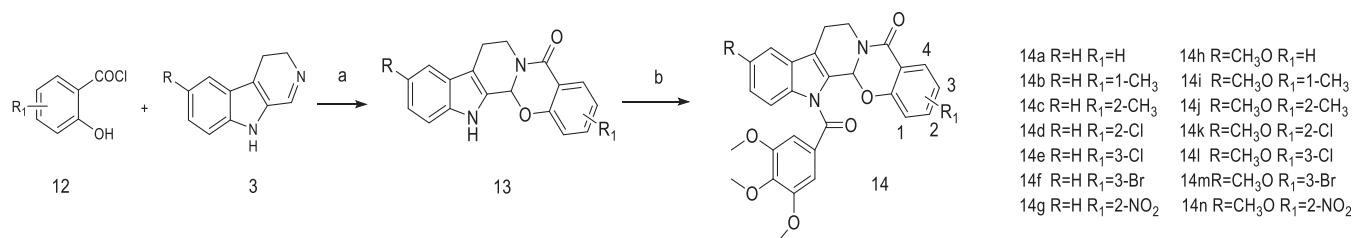
The scratch test was carried out in a six-well plate. After the cells were evenly filled in the six-well plate, used a 10 μl pipette tip to draw straight “wounds,” washed the suspended cells with phosphate buffered solution (PBS), and then added different concentrations of drugs to continue incubate for 48 h in an incubator. Observed and photographed the width of the “wound” at 0 and 48 h under the microscope. The migration rate calculated by the formula was used as the basis for the drug's ability to inhibit cell migration.

## 2.5 | Colony experiment

A single-cell suspension was spread on six-well plates and incubated in an incubator for 24 h. Cells were cultured with different concentrations of compound 14h (0, 0.75, 1.5, and 3 μmol/L) for 9 days, and the medium was changed every 3 days. Then the cells were fixed with 4% paraformaldehyde for 15 min. The colonies were washed with PBS and stained with 0.1% crystal violet for 15 min. After washed away excess crystal violet in PBS, observed the colony distribution in the six-well plate, and recorded the experimental results by taking pictures.

## 2.6 | Cell morphology analysis

Hoechst 33258 can label living cells. The cell culture in the experiment was similar to the colony experiment, incubating cells (12 h) and drug action (48 h) were in a six-well plate. Washed twice with PBS and fixed with 4% paraformaldehyde for 15 min. Then stained with 1 ml Hoechst 33258 solution in the dark for 10 min at 37°C. After



**SCHEME 2** Synthetic route of trimethoxyphenyl evodiamine derivative 14a-n

washed with PBS, the cells were observed with a fluorescence microscope (Olympus, Japan), and the detection wavelength was 350 nm.

## 2.7 | Cell cycle and apoptosis

### 2.7.1 | Apoptosis detection assay

HGC-27 cells were transplanted into six-well plates overnight, then different concentrations of compound **14h** dissolved in DMSO were added in triplicate for 48 h incubation and the control group was treated with 3% DMSO. After that, the cells were collected by trypsinization and washed twice with PBS. Then the cells resuspended in 400  $\mu$ l of 1 $\times$  binding buffer, 5  $\mu$ l of Annexin V-FITC, and 5  $\mu$ l of PI (BD Pharmingen, The United States). Finally, the stained cells were incubated at 25°C for 15 min in the dark and analyzed by flow cytometry.

### 2.7.2 | Cell cycle analysis

HGC-27 cells were transplanted into six-well plates overnight, then different concentrations of compound **14h** dissolved in DMSO were added in triplicate for 48 h incubation and the control group was treated with 3% DMSO. After that, the cells were washed with PBS and immobilized with a 70% ethanol solution for 12 h at 4°C. Then the cells were mixed with RNase A and propidium iodide staining solution (Beyotime, China). Finally, the stained cells were incubated at 25°C for 15 min in the dark and analyzed by flow cytometry.

## 2.8 | Determination of lactic acid content

HGC-27 cells were prepared as single-cell suspensions and cultured in six-well plates for 24 h (37°C, 5% CO<sub>2</sub>). Replaced with fresh culture medium containing different concentrations of compound **14h** (0, 0.75, 1.5, and 3  $\mu$ mol/L) and continue culturing for 48 h. The drug-free medium containing 3% DMSO was used as the control group. The working solution and cells in the lactic acid kit (Nanjing Jiancheng Bioengineering Institute, Nanjing, China) were vortexed and mixed and incubated at 37°C for 10 min. The reaction was terminated under the action of a terminator. The Wellscan MK-2 microplate reader measures the absorbance at 530 nm. Calculate the LD level according to the relevant formula. All experiments were repeated three times independently.

## 2.9 | Western blotting

The expression of the selected protein under the action of compound **14h** was analyzed by Western blotting. In a nutshell, under normoxic

conditions, HGC-27 cells were incubated in different concentrations (0, 0.75, 1.5, and 3  $\mu$ mol/L) for compound **14h** in triplicate for 48 h. Lyse the HGC-27 cells after 48 h of drug treatment in the six-well plate with lysis solution (phenylmethylsulfonyl fluoride [PMSF]: RIPA = 1:100). Aspirated the centrifuged supernatant and took 5  $\mu$ g to detect protein concentration with the BCA kit. An equal amount (30  $\mu$ g) of protein was separated by sodium dodecyl sulfate-polyacrylamide gel electrophoresis (8% gel, SDS-PAGE) and transferred to PVDF membrane. Blocked with 5% skim milk at room temperature for 2 h, and incubated the membrane with the corresponding antibody at 4°C overnight. TBST washes away excess antibody and then incubated with an anti-rabbit horseradish peroxidase-conjugated secondary antibody (VEGF [1:2000], Hexokinase [HK] [1:2000], pyruvate kinase [PK] [1:1000], and PFK [1:1000]) at room temperature for 1 h. Enhanced chemiluminescence system (Tanon6200, China) for visual detection of proteins. Each experiment was performed three times independently.

## 2.10 | Immunofluorescence

To investigate the effect of compound **14h** on tubulin, immunofluorescence was used to study the effect of synthetic compounds on cellular tubulin. In short, HGC-27 cells were treated with DMSO or different concentrations of compounds **14h** (0.75, 1.5, and 3  $\mu$ mol/L) for 48 h, and the dead cells were washed with PBS and fixed with 5% paraformaldehyde (PFA) at room temperature for 15 min, then Block for 30 min in PBS containing 1% bovine serine albumin (BSA). At room temperature, cells were incubated with Cy3 labeled goat anti-mouse IgG (1:250; Service Bio, CN) in a wet box for 1 h. Finally, DAPI (1:1000) stained the nuclei in the dark for 15 min, and the samples were mounted with an antifluorescence quencher. Sent the detection mechanism to test with a confocal laser microscope (Nikon C2 in Japan).

## 2.11 | Drug likeness

This study used the descriptor calculation module of MOE 2019. The ligand property calculation function of MOE 2019 can calculate molecular descriptors for all series of compounds (Table 3).

# 3 | RESULTS AND DISCUSSION

## 3.1 | Chemistry

A series of evodiamine derivatives were synthesized by splicing trimethoxyphenyl on the B ring or E ring of evodiamine (Figure 2). During the synthesis process, it was found that the yield of the product with a methoxy group at the 10-position was significantly higher than that of the unsubstituted product at the 10-position, and the yield of the compound with a halogen atom was also higher than that of the

Compound	LogP	Lip_acc	Lip_don	LogD (pH = 7)	LogS	TPSA	Weight
6a	2.64	4	2	2.64	-4.58	75.82	379.42
6b	3.39	5	1	3.39	-5.23	76.15	377.40
7a	2.50	5	2	2.50	-4.62	81.29	409.44
7b	3.25	6	1	3.25	-5.27	85.38	407.43
14a	5.50	6	0	5.50	-7.23	79.23	484.51
14b	5.72	6	0	5.72	-7.56	79.23	498.53
14c	6.0	6	0	6.0	-7.67	79.23	498.53
14d	6.21	6	0	6.21	-8.01	79.23	518.95
14e	6.18	6	0	6.18	-7.99	79.23	518.95
14f	6.35	6	0	6.35	-8.17	79.23	563.40
14g	5.62	6	0	5.62	-7.85	125.05	529.50
14h	5.37	7	0	5.37	-7.37	88.46	514.53
14i	5.59	7	0	5.59	-7.60	88.46	528.56
14j	5.87	7	0	5.87	-7.71	88.46	528.56
14k	6.08	7	0	6.08	-8.05	88.46	548.98
14l	6.05	7	0	6.05	-8.03	88.46	548.98
14m	6.22	7	0	6.22	-8.22	88.46	593.43
14n	5.49	7	0	5.49	-7.89	134.28	559.53

**TABLE 3** Physicochemical descriptors of compounds 6a–b, 7a–b, and 14a–n

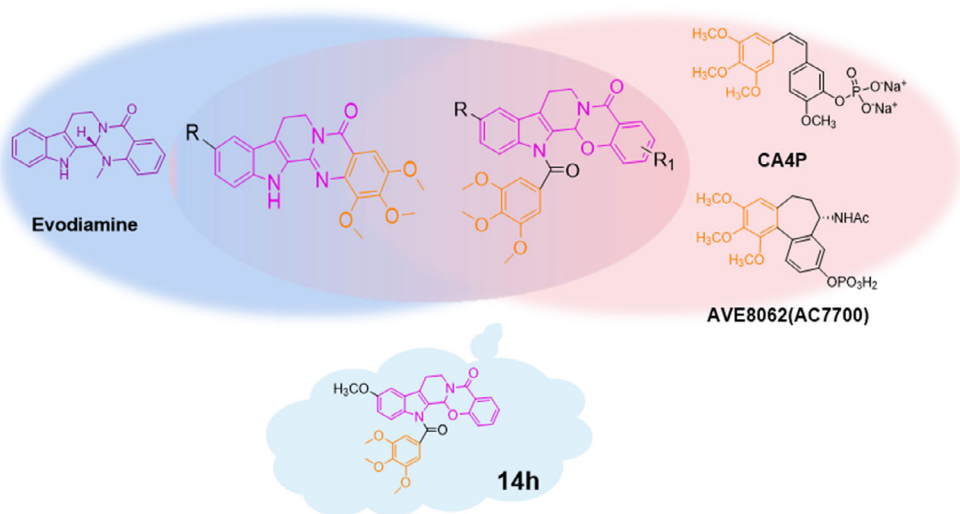


**FIGURE 2** The design and synthesis of trimethoxyphenyl evocarpine derivatives

methyl and nitro groups. The compound obtained through spectral data analysis was consistent with the expected design compound.

### 3.2 | In vitro antitumor cell proliferation experiment

In the experiment, 3-(4,5-dimethylthiazol-2-yl)-2,5-diphenyl tetrazolium bromide (MTT) assay was mainly used to detect the cytotoxicity of the drug. Evodiamine derivatives had good antiproliferative activity against five types of cancer cells, as shown in the data recorded in Table 4. The

different data we detected might be related to the modification of the structure of the E ring and the B ring, especially the B ring compounds were more sensitive to HGC-27 cells. Among them, 14a–c and 14i–j had significant effects, 14h ( $IC_{50} = 3.3 \pm 1.5 \mu M$ ) was the most prominent, even lower than evodiamine and 5-Fu, so compound 14h was selected for further study. In addition to its good antiproliferative activity against cancer cells, the toxicity of the compound to noncancer cells reflected its safety to a certain extent and was also an important indicator. All compounds were tested with GES-1 cells and did not show relatively high cytotoxicity. The results illustrated that these compounds were selective for the attack of cancer cells.

**TABLE 4** IC<sub>50</sub> value of compounds 6a–b, 7a–b, and 14a–n

Compound	IC <sub>50</sub> ± SD <sup>a</sup> (μM)					
	Bel-7402	A549	HCT-116	MCF-7	HGC-27	GES-1
6a	>100	>100	>100	>100	>100	>100
6b	35.4 ± 2.3	25.3 ± 1.2	64.3 ± 3.3	>100	38.2 ± 3.1	36.3 ± 1.8
7a	>100	>100	>100	>100	>100	>100
7b	>100	98.2 ± 2.3	>100	>100	88.2 ± 1.3	>100
14a	36.5 ± 1.2	17.3 ± 2.1	85.2 ± 2.3	80.8 ± 2.0	6.1 ± 2.5	>100
14b	>100	85.6 ± 3.2	>100	92.3 ± 1.3	7.3 ± 1.3	>100
14c	33.3 ± 2.3	13.5 ± 1.5	95.2 ± 2.3	95.7 ± 3.3	6.2 ± 2.6	>100
14d	>100	>100	>100	>100	92.9 ± 1.3	>100
14e	>100	>100	>100	>100	58.7 ± 2.0	>100
14f	>100	>100	>100	>100	68.0 ± 3.2	>100
14g	>100	>100	>100	>100	90.2 ± 1.5	>100
14h	28.1 ± 1.3	8.5 ± 2.1	80.8 ± 2.3	72.3 ± 1.5	3.3 ± 1.5	>100
14i	8.2 ± 3.3	29.3 ± 1.3	91.2 ± 1.5	90.2 ± 3.3	7.3 ± 2.1	>100
14j	>100	11.9 ± 2.3	>100	85.3 ± 1.6	6.7 ± 1.4	>100
14k	>100	>100	>100	>100	90.2 ± 2.0	>100
14l	>100	>100	>100	>100	49.3 ± 1.3	>100
14m	>100	>100	>100	>100	10.7 ± 4.3	>100
14n	>100	>100	>100	>100	85.0 ± 1.3	>100
Evodiamine	38.1 ± 1.3	>100	>100	>100	22.6 ± 3.2	25.6 ± 2.2
5-Fu	36.9 ± 1.2	61.7 ± 5.4	32.6 ± 2.1	57.9 ± 3.7	18.9 ± 2.7	>100

<sup>a</sup>Data are the average of three independent assays; SD, standard deviation.

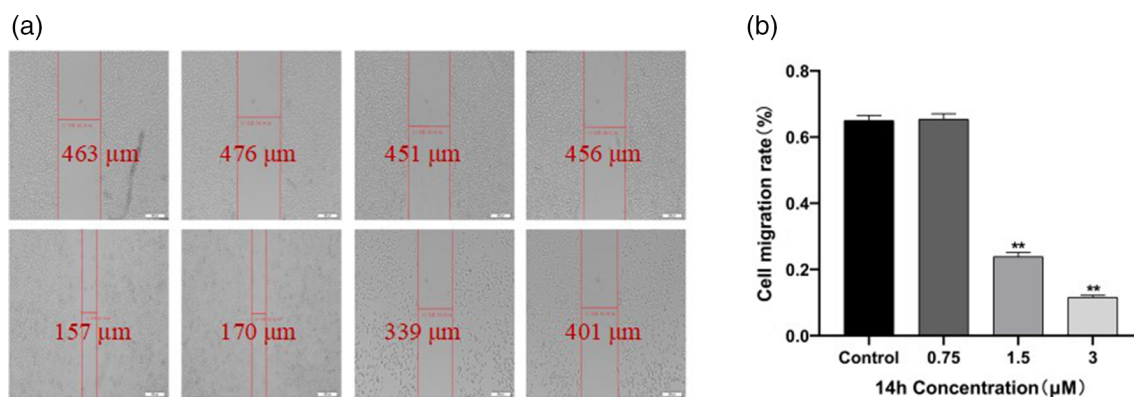


**FIGURE 3** Detection of the ability of drugs to inhibit cell migration. Compound 14h inhibited the migration of HGC-27 cells. (a) The width of the “wound” after 0 and 48 h was observed and photographed under a microscope; (b) HGC-27 cell mobility was negatively correlated with compound 14h. Error basis showed the SD, “\*\*\*”  $p < .01$ , compared with the control group

### 3.3 | Cell migration and colony formation

The scratch experiment explored the effect of compound 14h on the migration of HGC-27 cells. As shown in Figure 3, the scratch area of the control group healed almost completely after 48 h, while the healing rate of the scratch in the drug-treated group was significantly slowed down (Figure 3(a)). The migration rate (Figure 3(b)) could

intuitively see the inhibitory effect was concentration-dependent. Besides, The colonies stained with crystal violet reflected the effects of different concentrations of drugs in a six-well plate. Statistical results (Figure 4) showed that the cell proliferation of the drug group was more or less inhibited compared with the control group, and the high concentration group was almost completely suppressed. Reflected the good antiproliferative activity against HGC-27 cells in compound 14h.

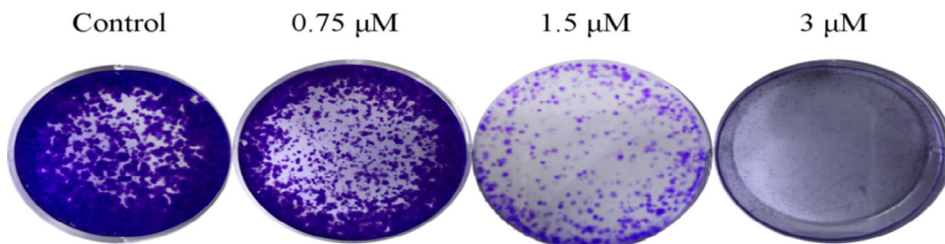


**FIGURE 4** Compound 14h inhibited the proliferation of HGC-27 cells

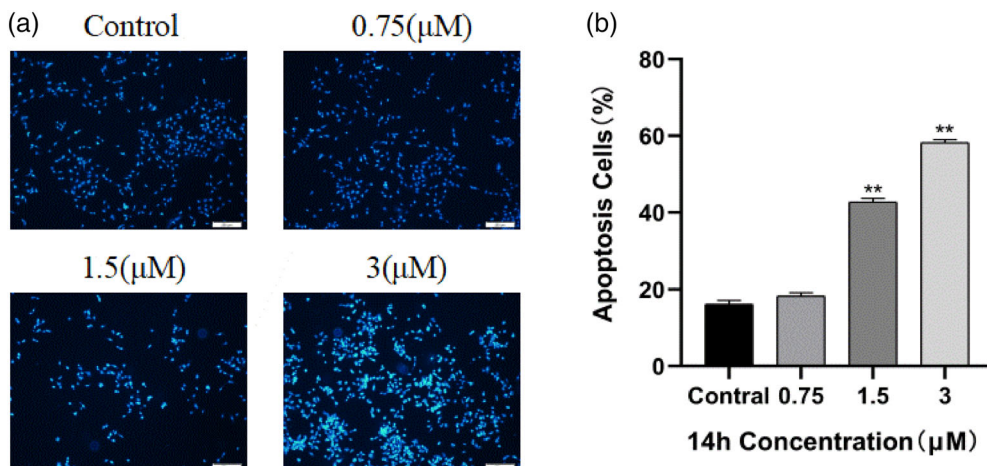


**FIGURE 5** Cell morphology analysis. Hoechst staining was used to observe the effect of HGC-27 cells treated with compound 14h on apoptosis. (a) Cell chromatogram under the fluorescence microscope. (b) There was a positive correlation between the total amount of apoptosis and the concentration of compound 14h. Error basis showed the SD, \*\*\*\* $p < .01$ , compared with the control group

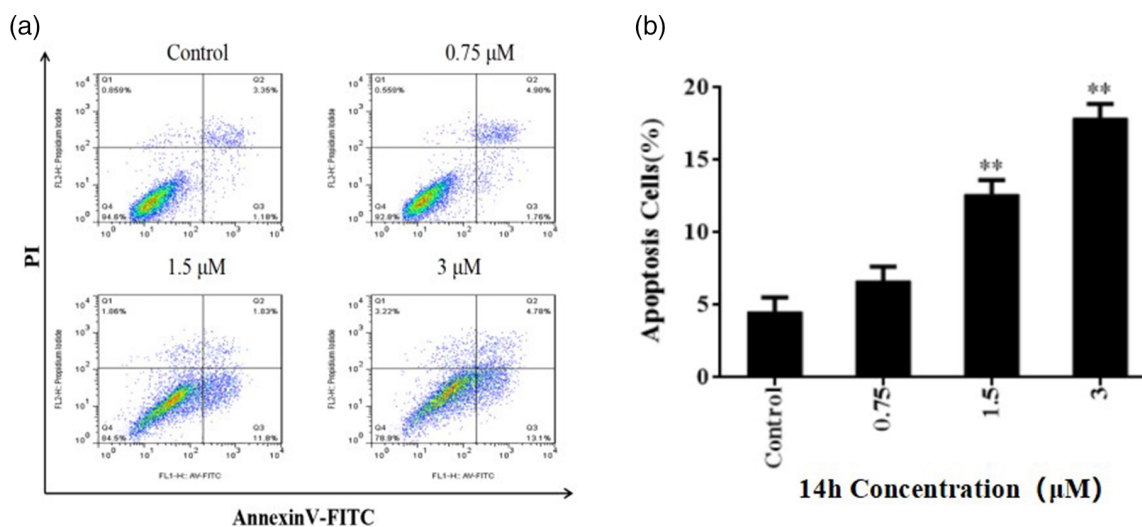


**FIGURE 6** Apoptosis analysis. Effect of compound 14h on apoptosis of HGC-27 cells after 48 h treatment. (a) Flow Jo software was used to calculate the number of apoptotic cells. Q1, Q2, Q3, and Q4, respectively, represent cell fragments, early apoptotic cells, late apoptotic cells, and normal living cells. (b) There was a positive correlation between the total amount of apoptosis and the concentration of compound 14h. Error basis showed the SD, \*\*\*\* $p < .01$ , compared with the control group

### 3.4 | Apoptosis and cycle experiment

After 48 h of drug action, the results (Figure 5) showed that HGC-27 cells showed chromatin condensation and nuclear fragmentation, marking cell apoptosis. Flow cytometry analysis of the combination of

cells with Annexin V-FITC and PI showed changes in the proportion of apoptosis. Compared with the control group (4.53%), the apoptosis rates of drug action were 6.66%, 13.63%, and 17.88% (Figure 6), which showed a certain concentration dependence. These results proved that compound 14h can induce apoptosis of HGC-27 cells,

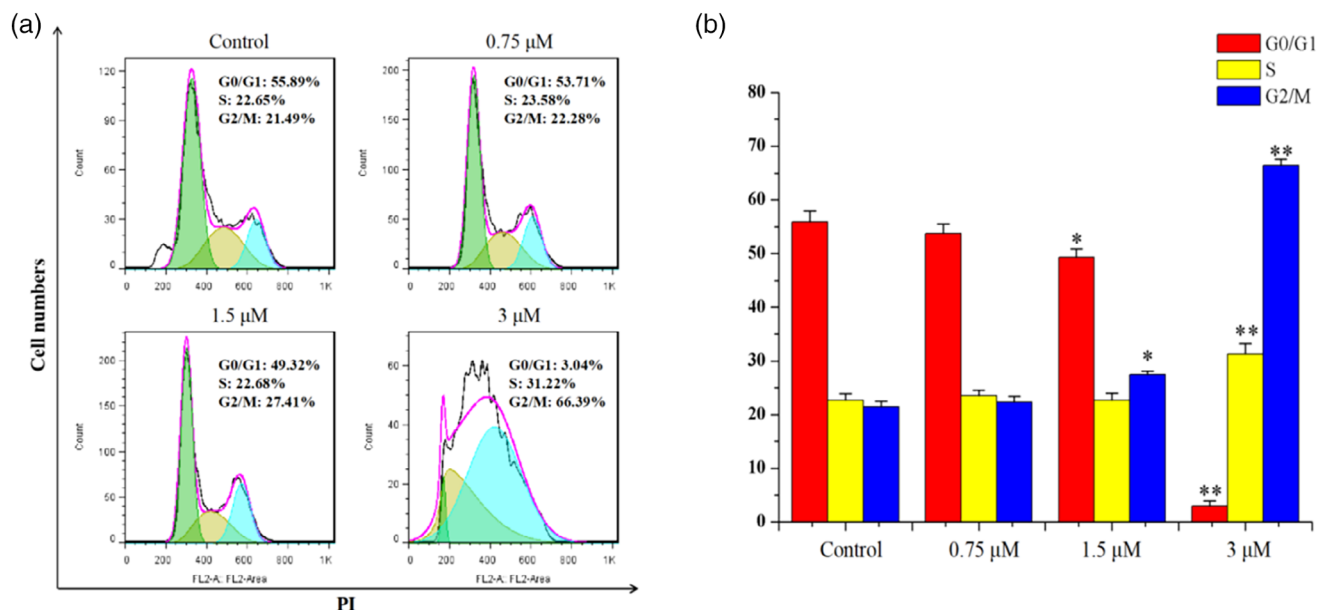


**FIGURE 7** Cell cycle analysis. The effect of compound **14h** on the cell cycle distribution of HGC-27. (a) Flow cytometry analysis showed that the distribution of the HGC-27 cell cycle was affected after **14h** treatment for 48 h. The percentage of different stages of the cell cycle was calculated by flow software. (b) The percentage of G1/G0, G2/M, and S phase was plotted by origin8 software. \*\*\*\* $p < .05$ , \*\*\*\*\* $p < .01$

**TABLE 5** Determination of lactate content in HGC-27 cells treated with different concentrations for **14h** comparison with control group: \*\*\*\*\* $p < .01$

Group	Concentration(μmol/L)	Lactate content(mmol/L)
Control	—	13.251 ± 0.005**
<b>14h</b>	0.75	9.660 ± 0.005**
	1.5	8.732 ± 0.006**
	3	7.428 ± 0.009**

and its antiproliferative effect was closely related to their strong proapoptotic activity.

To investigate the effect of compound **14h** on the cycle of HGC-27 cells, we used flow cytometry to detect the cells after 48 h of drug action. The cell cycle stage had a significant change (Figure 7), in which the cell cycle distribution changes the most when the drug concentration is 3 μM. The number of cells in the G2/M phase increased to 66.39%, the number of cells in the G0/G1 phase decreased significantly to 3.04%, and there was no significant difference in the percentage of cells in the s phase (Figure 7(b)). Therefore, compound **14h** inhibited the proliferation of HGC-27 cells by inducing G2/M phase arrest, which was consistent with the cytotoxicity test results.

### 3.5 | Western blot analysis of the effect on glycolysis

Lactic acid is closely related to intracellular energy metabolism. Compared with the control group (Table 5), the lactic acid content of different concentrations of drugs decreased after 24 h, and the highest

concentration decreased the most. Phosphofructose kinase and hexokinase played a key role in the glycolysis pathway. If the drug could inhibit the expression of these two enzymes, it might be possible to inhibit glycolysis by blocking the energy supply of the cells, thereby starving the tumor cells. To verify this conjecture, we analyzed the compound **14h** by immunoblotting. Western blot analysis (WB) results (Figure 8) showed that compound **14h** had a certain degree of inhibitory effect on the expression of VEGF, HK, PK, and PFK. Compared with the control group, the protein expression in the drug-treated group decreased significantly, indicating that these proteins could be down-regulated at compound **14h**. This suggested that compound **14h** might kill tumors by inhibiting VEGF and glycolysis.

### 3.6 | Immunofluorescence and molecular docking simulation

The control group's tubulin spread out around, showing a network structure, but the cellular tubulin of the drug action gathered around the cell periphery (Figure 9), indicating that the aggregation of microtubules and the formation of the spindle were disturbed, hindering the mitosis of the cells leading to abnormal spindles. It was suggested that compound **14h** could inhibit the tubulin assembly of HGC-27 cells.

### 3.7 | Drug likeness

The log *P*, Lipinski's acceptors (lip-acc), Lipinski's donors (lip-don), log *D* (pH = 7), molecular weight, and total polar specific surface area

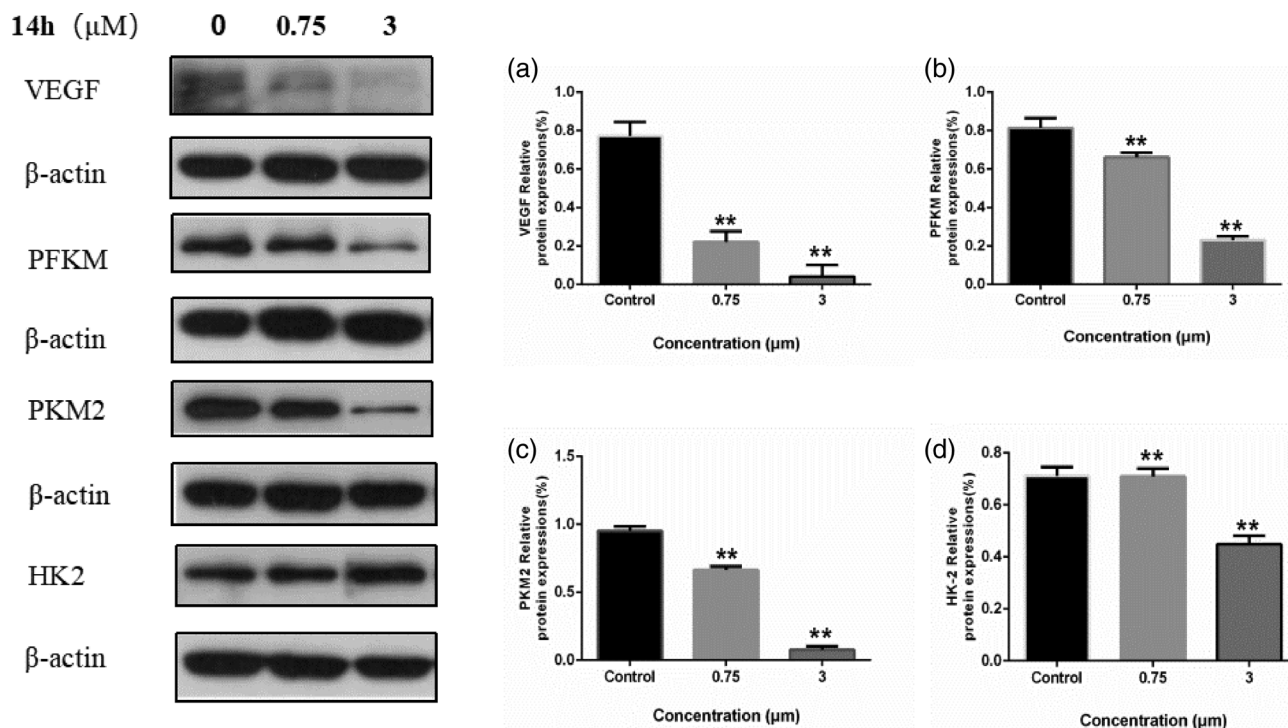


**FIGURE 8** Western blot data analysis. The expression of VEGF, PFKM, PKM2, and HK-2 in HGC-27 cells was influenced by the compound 14h. The Western blot results were quantitatively analyzed by calculating the ratio of the experimental group to the control group. Representative photos of four independent experiments are shown. Error basis showed the SD, “\*\*”  $p < .01$ , compared with the control group

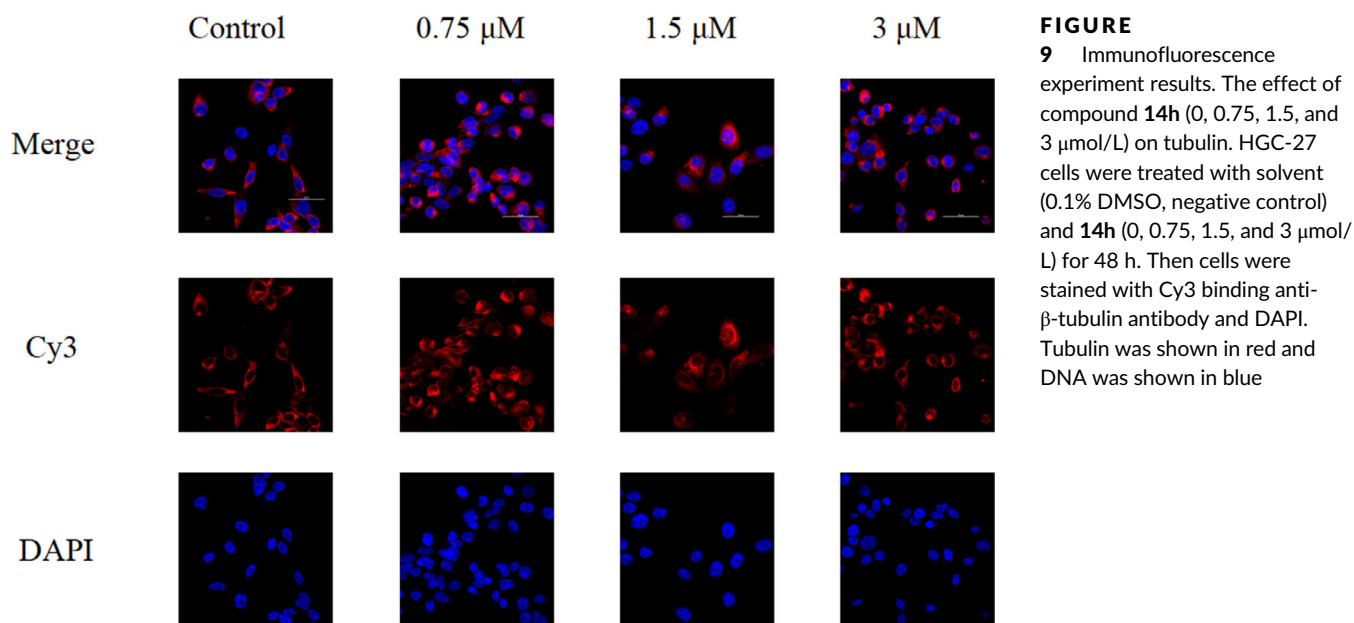


**FIGURE 9** Immunofluorescence experiment results. The effect of compound 14h (0, 0.75, 1.5, and 3 μmol/L) on tubulin. HGC-27 cells were treated with solvent (0.1% DMSO, negative control) and 14h (0, 0.75, 1.5, and 3 μmol/L) for 48 h. Then cells were stained with Cy3 binding anti-β-tubulin antibody and DAPI. Tubulin was shown in red and DNA was shown in blue

(TPSA) were calculated to test the pharmaceutical properties of the synthesized trimethoxyphenyl evodiamine derivatives (Aziz, Saeed, Khan, Afridi, & Jabeen, 2020a; Aziz, Saeed, Khan, Afridi, Jabeen, Ashfaq Ur, & Hashim, 2020b; Lipinski et al., 2001). These descriptors have predictive power in evaluating the likelihood of a drug being made into a drug. Drug-like molecules must have log  $P$  (the logarithm of the octanol/water partition coefficient)  $\leq 5$ , total polar specific

surface area (TPSA)  $< 140 \text{ \AA}^2$ , molecular weight  $\leq 500$ , number of hydrogen bond donors  $\leq 5$ , and hydrogen bond acceptor  $\leq 10$  as per Lipinski's RO5. The compounds conform to the drug-like principle to provide a basis for its preparation. The detailed results of the drug similarity of the 18 compounds are listed in Table 3. According to Lipinski's rule, the bioavailability of 14h may not be as expected, and more experiments are needed to explore and modify.

## 4 | CONCLUSION

By modifying the structure of ethylenediamine, a series of compounds containing 3,4,5-trimethoxyphenyl scaffolds were obtained, and their activities were tested in vitro. From the MTT results, we found that compound **14h** had high cytotoxicity to five kinds of cancer cells, especially HGC-27 cells. Subsequent experiments further confirmed that compound **14h** could inhibit cell proliferation and migration, and induce G2/M phase arrest to inhibit the proliferation of HGC-27 cells, which is consistent with the results of the cytotoxicity experiment. Besides, **14h** could inhibit microtubule assembly and might kill tumor cells by inhibiting VEGF and glycolysis. In summary, compound **14h** might be a potential drug candidate for the treatment of gastric cancer, but its mechanism was still unclear and deserves further study.

### ACKNOWLEDGMENTS

This work was financially supported by Hunan Provincial Key Laboratory of Tumor Microenvironment Responsive Drug Research (Approval number: 2019-56), Hunan Province Cooperative Innovation Center for Molecular Target New Drug Study, The Natural Science Foundation of Hunan Province (Approval number: 2020JJ4534), and Hunan Postgraduate Research and Innovation Project (Approval number: CX20190751).

### CONFLICT OF INTEREST

The authors declare no conflicts of interest.

### DATA AVAILABILITY STATEMENT

All data included in this study are available upon request by contact with the corresponding author.

### ORCID

Zhi-Zhong Xie  <https://orcid.org/0000-0003-3365-0379>

Guotao Tang  <https://orcid.org/0000-0001-9673-4727>

### REFERENCES

- Aziz, H., Saeed, A., Khan, M. A., Afridi, S., & Jabeen, F. (2020a). Synthesis, characterization, antimicrobial, antioxidant and computational evaluation of N-acyl-morpholine-4-carbothioamides. *Molecular Diversity*, *https://doi.org/10.1007/s11030-020-10054-w*
- Aziz, H., Saeed, A., Khan, M. A., Afridi, S., Jabeen, F., Ashfaq Ur, R., & Hashim, M. (2020b). Novel N-acyl-1H-imidazole-1-carbothioamides: Design, synthesis, biological and computational studies. *Chemistry & Biodiversity*, *17*(3), e1900509. <https://doi.org/10.1002/cbdv.201900509>
- Bak, E. J., Park, H. G., Kim, J. M., Kim, J. M., Yoo, Y. J., & Cha, J. H. (2010). Inhibitory effect of evodiamine alone and in combination with rosiglitazone on in vitro adipocyte differentiation and in vivo obesity related to diabetes. *International Journal of Obesity*, *34*(2), 250–260. <https://doi.org/10.1038/ijo.2009.223>
- Belleri, M., Ribatti, D., Nicoli, S., Cotelli, F., Forti, L., Vannini, V., Stivala, L. A., & Presta, M. (2005). Antiangiogenic and vascular-targeting activity of the microtubule-destabilizing trans-resveratrol derivative 3,5,4'-trimethoxystilbene. *Molecular Pharmacology*, *67*(5), 1451–1459. <https://doi.org/10.1124/mol.104.009043>
- Bothwell, K. D., Folaron, M., & Seshadri, M. (2016). Preclinical activity of the vascular disrupting agent OXi4503 against head and neck cancer. *Cancers (Basel)*, *8*(1), 1–12. <https://doi.org/10.3390/cancers8010011>
- Chen, Q., Liu, G., Liu, S., Su, H., Wang, Y., Li, J., & Luo, C. (2018). Remodeling the tumor microenvironment with emerging nanotherapeutics. *Trends in Pharmacological Sciences*, *39*(1), 59–74. <https://doi.org/10.1016/j.tips.2017.10.009>
- Chen, T. C., Chien, C. C., Wu, M. S., & Chen, Y. C. (2016). Evodiamine from *Evodia rutaecarpa* induces apoptosis via activation of JNK and PERK in human ovarian cancer cells. *Phytomedicine*, *23*(1), 68–78. <https://doi.org/10.1016/j.phymed.2015.12.003>
- Chien, C. C., Wu, M. S., Shen, S. C., Ko, C. H., Chen, C. H., Yang, L. L., & Chen, Y. C. (2014). Activation of JNK contributes to evodiamine-induced apoptosis and G2/M arrest in human colorectal carcinoma cells: A structure-activity study of evodiamine. *PLoS One*, *9*(6), e99729. <https://doi.org/10.1371/journal.pone.0099729>
- Fang, C., Zhang, J., Qi, D., Fan, X., Luo, J., Liu, L., & Tan, Q. (2014). Evodiamine induces G2/M arrest and apoptosis via mitochondrial and endoplasmic reticulum pathways in H446 and H1688 human small-cell lung cancer cells. *PLoS One*, *9*(12), e115204. <https://doi.org/10.1371/journal.pone.0115204>
- Gavaraskar, K., Dhulap, S., & Hirwani, R. R. (2015). Therapeutic and cosmetic applications of evodiamine and its derivatives: A patent review. *Fitoterapia*, *106*, 22–35. <https://doi.org/10.1016/j.fitote.2015.07.019>
- Gaya, A. M., & Rustin, G. J. (2005). Vascular disrupting agents: A new class of drug in cancer therapy. *Clinical Oncology (Royal College of Radiologists)*, *17*(4), 277–290. <https://doi.org/10.1016/j.clon.2004.11.011>
- Herdman, C. A., Strecker, T. E., Tanpure, R. P., Chen, Z., Winters, A., Gerberich, J., Liu, L., Hamel, E., Mason, R. P., Chaplin, D. J., Trawick, M. L., & Pinney, K. G. (2016). Synthesis and biological evaluation of benzocyclooctene-based and indene-based anticancer agents that function as inhibitors of tubulin polymerization. *MedChemComm*, *7*(12), 2418–2427. <https://doi.org/10.1039/C6MD00459H>
- Hong, J. Y., Park, S. H., Min, H. Y., Park, H. J., & Lee, S. K. (2014). Antiproliferative effects of evodiamine in human lung cancer cells. *Journal of Cancer Prevention*, *19*(1), 7–13. <https://doi.org/10.15430/jcp.2014.19.1.7>
- Hu, C. Y., Wu, H. T., Su, Y. C., Lin, C. H., Chang, C. J., & Wu, C. L. (2017). Evodiamine exerts an anti-hepatocellular carcinoma activity through a WWOX-dependent pathway. *Molecules*, *22*(7), 1–8. <https://doi.org/10.3390/molecules22071175>
- Huang, J., Chen, Z. H., Ren, C. M., Wang, D. X., Yuan, S. X., Wu, Q. X., Chen, Q. Z., Zeng, Y. H., Shao, Y., Li, Y., Wu, K., Yu, Y., Sun, W. J., & He, B. C. (2015). Antiproliferation effect of evodiamine in human colon cancer cells is associated with IGF-1/HIF-1 $\alpha$  downregulation. *Oncology Reports*, *34*(6), 3203–3211. <https://doi.org/10.3892/or.2015.4309>
- Jaiswal, P. K., Goel, A., & Mittal, R. D. (2015). Survivin: A molecular biomarker in cancer. *The Indian Journal of Medical Research*, *141*(4), 389–397. <https://doi.org/10.4103/0971-5916.159250>
- Jiang, Y. N. (2015). The study of evodiamine to interfere the glycometabolism of tumours. *Guangzhou University of Chinese Medicine*, *10*(3), 1–61.
- Khan, M., Bi, Y., Qazi, J. I., Fan, L., & Gao, H. (2015). Evodiamine sensitizes U87 glioblastoma cells to TRAIL via the death receptor pathway. *Molecular Medicine Reports*, *11*(1), 257–262. <https://doi.org/10.3892/mmr.2014.2705>
- Lee, J., Kim, S. J., Choi, H., Kim, Y. H., Lim, I. T., Yang, H. M., Lee, C. S., Kang, H. R., Ahn, S. K., Moon, S. K., Kim, D. H., Lee, S., Choi, N. S., & Lee, K. J. (2010). Identification of CKD-516: A potent tubulin polymerization inhibitor with marked antitumor activity against murine and human solid tumors. *Journal of Medicinal Chemistry*, *53*(17), 6337–6354. <https://doi.org/10.1021/jm1002414>
- Li, L., Jiang, S., Li, X., Liu, Y., Su, J., & Chen, J. (2018). Recent advances in trimethoxyphenyl (TMP) based tubulin inhibitors targeting the

- colchicine binding site. *European Journal of Medicinal Chemistry*, 151, 482–494. <https://doi.org/10.1016/j.ejmech.2018.04.011>
- Liang, W., Lai, Y., Zhu, M., Huang, S., Feng, W., & Gu, X. (2016). Combretastatin A4 regulates proliferation, migration, invasion, and apoptosis of thyroid cancer cells via PI3K/Akt signaling pathway. *Medical Science Monitor*, 22, 4911–4917. <https://doi.org/10.12659/msm.898545>
- Liao, J. F., Chiou, W. F., Shen, Y. C., Wang, G. J., & Chen, C. F. (2011). Anti-inflammatory and anti-infectious effects of *Evodia rutaecarpa* (Wuzhuyu) and its major bioactive components. *Chinese Medicine*, 6(1), 6. <https://doi.org/10.1186/1749-8546-6-6>
- Lipinski, C. A., Lombardo, F., Dominy, B. W., & Feeney, P. J. (2001). Experimental and computational approaches to estimate solubility and permeability in drug discovery and development settings. *Advanced Drug Delivery Reviews*, 46(1–3), 3–26. [https://doi.org/10.1016/s0169-409x\(00\)00129-0](https://doi.org/10.1016/s0169-409x(00)00129-0)
- LoRusso, P. M., Gadgeel, S. M., Wozniak, A., Barge, A. J., Jones, H. K., DelProposto, Z. S., DeLuca, P. A., Evelhoch, J. L., Boerner, S. A., & Wheeler, C. (2008). Phase I clinical evaluation of ZD6126, a novel vascular-targeting agent, in patients with solid tumors. *Investigational New Drugs*, 26(2), 159–167. <https://doi.org/10.1007/s10637-008-9112-9>
- McKeage, M. J., & Baguley, B. C. (2010). Disrupting established tumor blood vessels: An emerging therapeutic strategy for cancer. *Cancer*, 116(8), 1859–1871. <https://doi.org/10.1002/cncr.24975>
- Nguyen, T. T., Lomberget, T., Tran, N. C., Colomb, E., Nachtergaele, L., Thoret, S., Dubois, J., Guillaume, J., Abdayem, R., Haftek, M., & Barret, R. (2012). Synthesis and biological evaluation of novel heterocyclic derivatives of combretastatin A-4. *Bioorganic & Medicinal Chemistry Letters*, 22(23), 7227–7231. <https://doi.org/10.1016/j.bmcl.2012.09.047>
- Nowak, A. K., Brown, C., Millward, M. J., Creaney, J., Byrne, M. J., Hughes, B., Kremmidiotis, G., Bibby, D. C., Leske, A. F., Mitchell, P. L. R., Pavlakis, N., Boyer, M., & Stockler, M. R. (2013). A phase II clinical trial of the vascular disrupting agent BNC105P as second line chemotherapy for advanced malignant pleural mesothelioma. *Lung Cancer*, 81(3), 422–427. <https://doi.org/10.1016/j.lungcan.2013.05.006>
- Porcu, E., Bortolozzi, R., Basso, G., & Viola, G. (2014). Recent advances in vascular disrupting agents in cancer therapy. *Future Medicinal Chemistry*, 6(13), 1485–1498. <https://doi.org/10.4155/fmc.14.104>
- Quan, H., Xu, Y., & Lou, L. (2008). p38 MAPK, but not ERK1/2, is critically involved in the cytotoxicity of the novel vascular disrupting agent combretastatin A4. *International Journal of Cancer*, 122(8), 1730–1737. <https://doi.org/10.1002/ijc.23262>
- Rasul, A., Yu, B., Zhong, L., Khan, M., Yang, H., & Ma, T. (2012). Cytotoxic effect of evodiamine in SGC-7901 human gastric adenocarcinoma cells via simultaneous induction of apoptosis and autophagy. *Oncology Reports*, 27(5), 1481–1487. <https://doi.org/10.3892/or.2012.1694>
- Sessa, C., Lorusso, P., Tolcher, A., Farace, F., Lassau, N., Delmonte, A., Braghetti, A., Bahleda, R., Cohen, P., Hospitel, M., Veyrat-Follet, C., & Soria, J. C. (2013). Phase I safety, pharmacokinetic and pharmacodynamic evaluation of the vascular disrupting agent ombrabulin (AVE8062) in patients with advanced solid tumors. *Clinical Cancer Research*, 19(17), 4832–4842. <https://doi.org/10.1158/1078-0432.CCR-13-0427>
- Shen, H., Zhao, S., Xu, Z., Zhu, L., Han, Y., & Ye, J. (2015). Evodiamine inhibits proliferation and induces apoptosis in gastric cancer cells. *Oncology Letters*, 10(1), 367–371. <https://doi.org/10.3892/ol.2015.3153>
- Siemann, D. W., Chaplin, D. J., & Horsman, M. R. (2017). Realizing the potential of vascular targeted therapy: The rationale for combining vascular disrupting agents and anti-angiogenic agents to treat cancer. *Cancer Investigation*, 35(8), 519–534. <https://doi.org/10.1080/07357907.2017.1364745>
- Siemann, D. W., & Shi, W. (2004). Efficacy of combined antiangiogenic and vascular disrupting agents in treatment of solid tumors. *International Journal of Radiation Oncology, Biology, Physics*, 60(4), 1233–1240. <https://doi.org/10.1016/j.ijrobp.2004.08.002>
- Tan, Q., & Zhang, J. (2016). Evodiamine and its role in chronic diseases. *Advances in Experimental Medicine and Biology*, 929, 315–328. [https://doi.org/10.1007/978-3-319-41342-6\\_14](https://doi.org/10.1007/978-3-319-41342-6_14)
- Yan, J., Pang, Y., Sheng, J., Wang, Y., Chen, J., Hu, J., & Li, X. (2015). A novel synthetic compound exerts effective anti-tumour activity in vivo via the inhibition of tubulin polymerisation in A549 cells. *Biochemical Pharmacology*, 97(1), 51–61. <https://doi.org/10.1016/j.bcp.2015.07.008>
- Yang, L., Liu, X., Wu, D., Zhang, M., Ran, G., Bi, Y., & Huang, H. (2014). Growth inhibition and induction of apoptosis in SGC7901 human gastric cancer cells by evodiamine. *Molecular Medicine Reports*, 9(4), 1147–1152. <https://doi.org/10.3892/mmr.2014.1924>
- Yang, L. V. (2017). Tumor microenvironment and metabolism. *International Journal of Molecular Sciences*, 18(12), 1–6. <https://doi.org/10.3390/ijms18122729>
- Zhang, C., Zhou, S. S., Li, X. R., Wang, B. M., Lin, N. M., Feng, L. Y., Zhang, D. Y., Zhang, L. H., Wang, J. B., & Pan, J. P. (2013). Enhanced antitumor activity by the combination of dasatinib and combretastatin A-4 in vitro and in vivo. *Oncology Reports*, 29(6), 2275–2282. <https://doi.org/10.3892/or.2013.2405>
- Zhao, L. C., Li, J., Liao, K., Luo, N., Shi, Q. Q., Feng, Z. Q., & Chen, D. L. (2015). Evodiamine induces apoptosis and inhibits migration of HCT-116 human colorectal cancer cells. *International Journal of Molecular Sciences*, 16(11), 27411–27421. <https://doi.org/10.3390/ijms161126031>

## SUPPORTING INFORMATION

Additional supporting information may be found online in the Supporting Information section at the end of this article.

**How to cite this article:** Peng Y, Xiong R, Li Z, et al. Design, synthesis, and biological evaluation of 3',4',5'-trimethoxy evodiamine derivatives as potential antitumor agents. *Drug Dev Res*. 2021;1–12. <https://doi.org/10.1002/ddr.21806>